

**Supplementary Information**

**UV-Vis determination of acetate in ethanol electrolysis for  
renewable hydrogen production**

Zuyao Li,<sup>1,+</sup> Jing Li,<sup>1,+</sup> Chaoyang Jiang,<sup>1</sup> Guiyun Liu,<sup>1</sup> Zihan Fang,<sup>1</sup> Zhenchen Tang,<sup>1</sup>  
Huanhao Chen,<sup>1</sup> Hai Cao,<sup>1</sup> Feng Zeng<sup>1,\*</sup>

<sup>1</sup>State Key Laboratory of Materials-Oriented Chemical Engineering, College of  
Chemical Engineering, Nanjing Tech University, Nanjing, Jiangsu 211816, China

<sup>+</sup>These authors contributed equally.

\*Corresponding authors: [zeng@njtech.edu.cn](mailto:zeng@njtech.edu.cn)

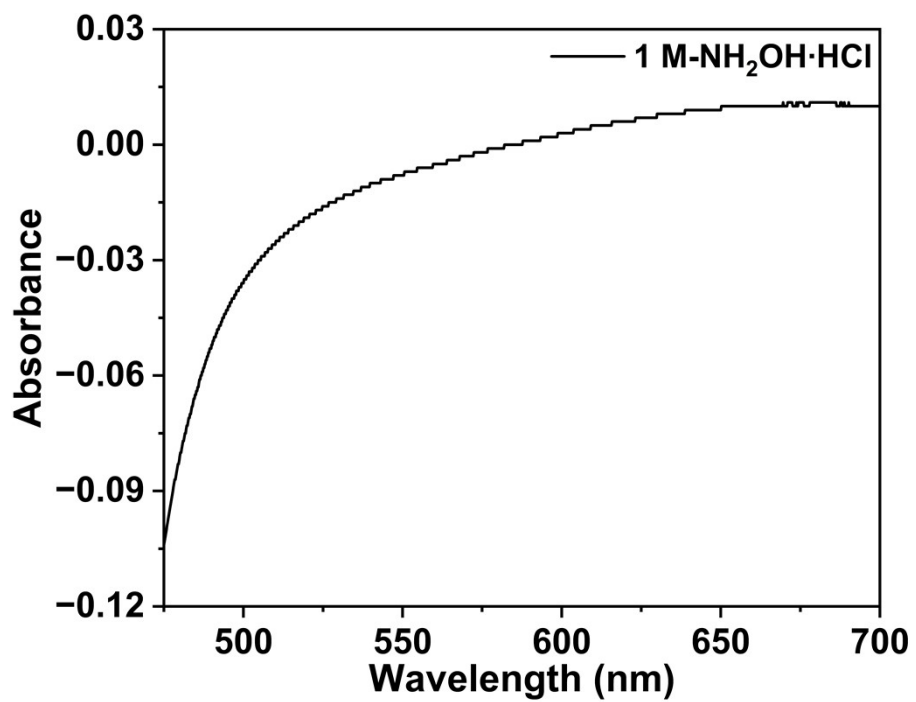


**Fig. S1** UV-Vis spectra of NH<sub>2</sub>OH·HCl solution.

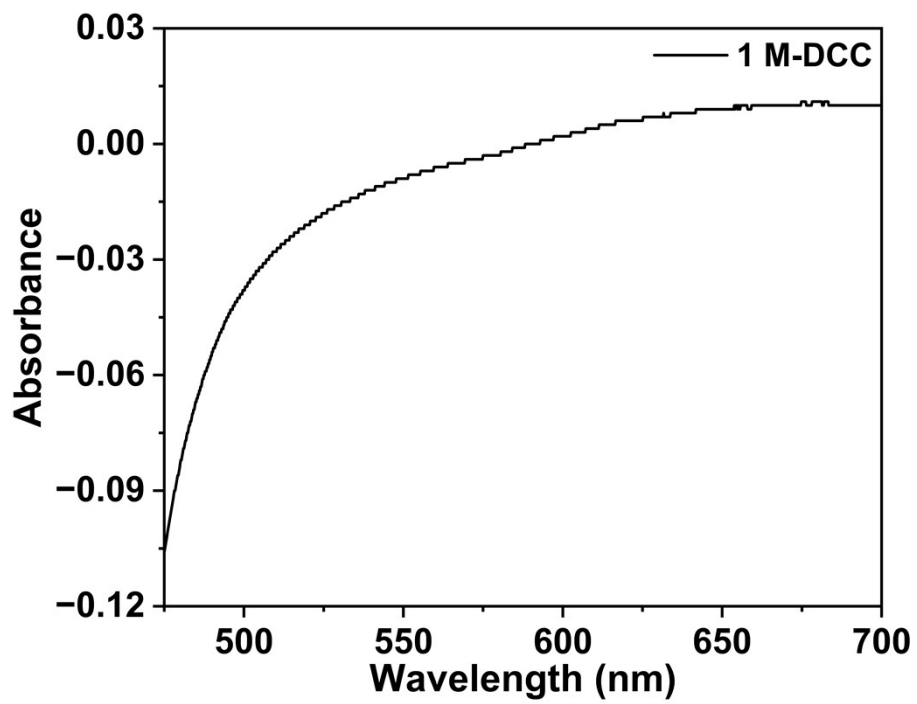


Fig. S2 UV-Vis spectra of DCC solution.

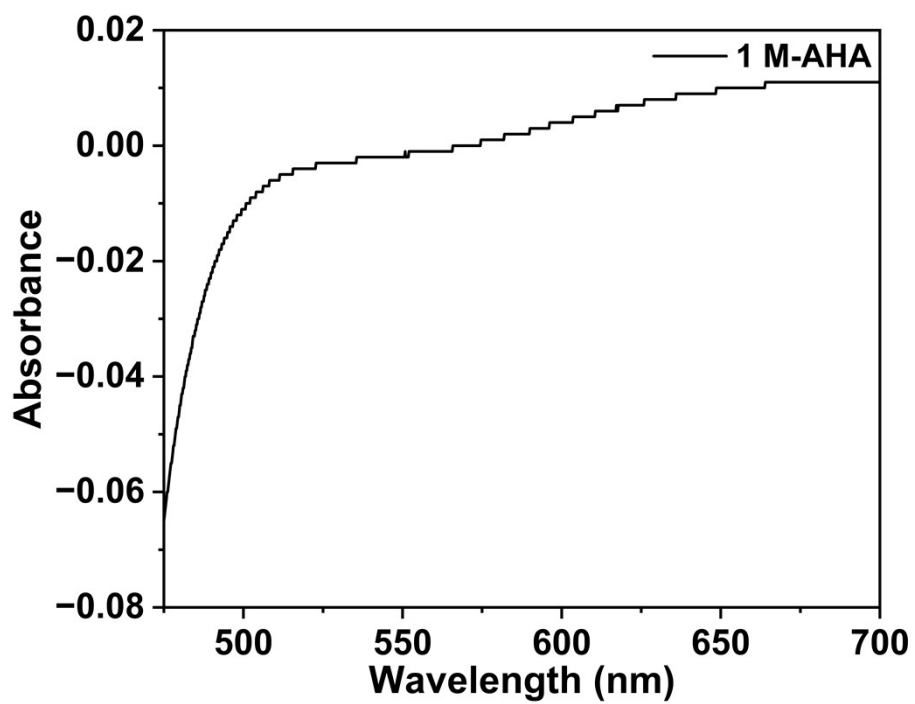


Fig. S3 UV-Vis spectra of AHA solution.

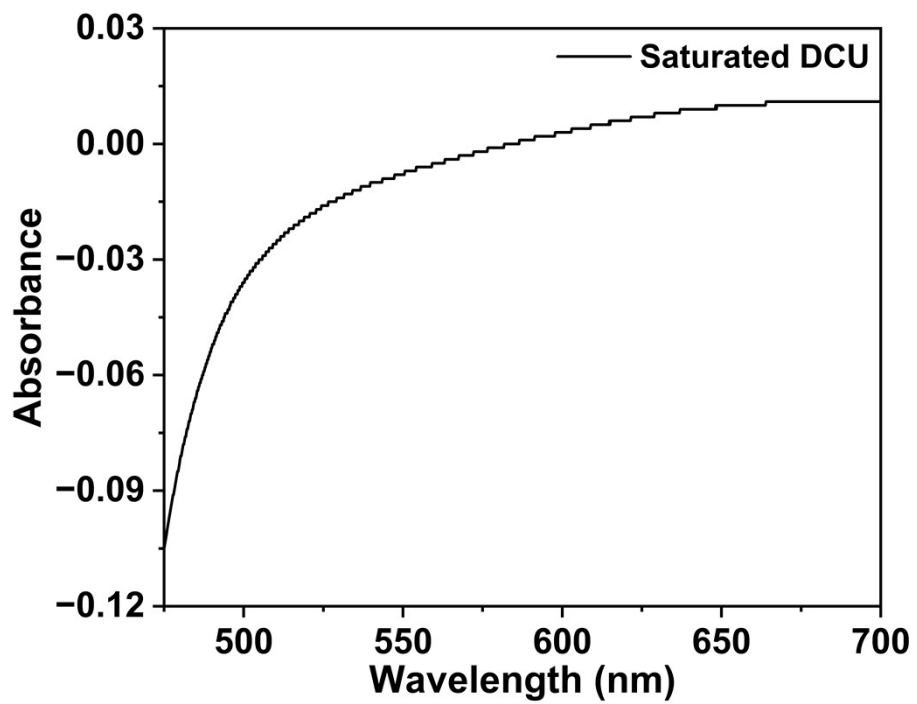
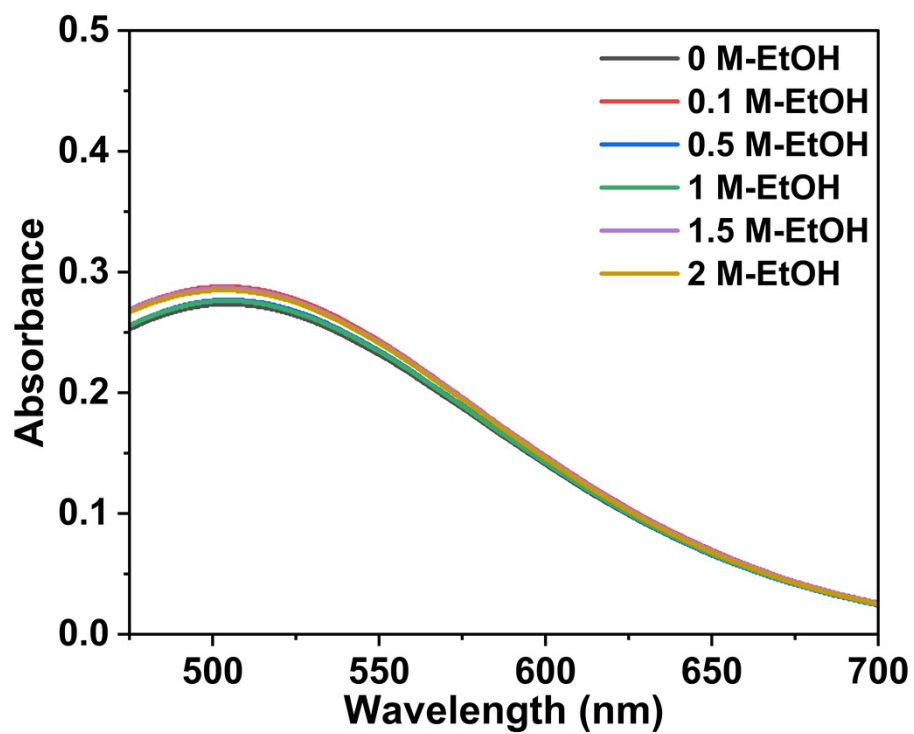
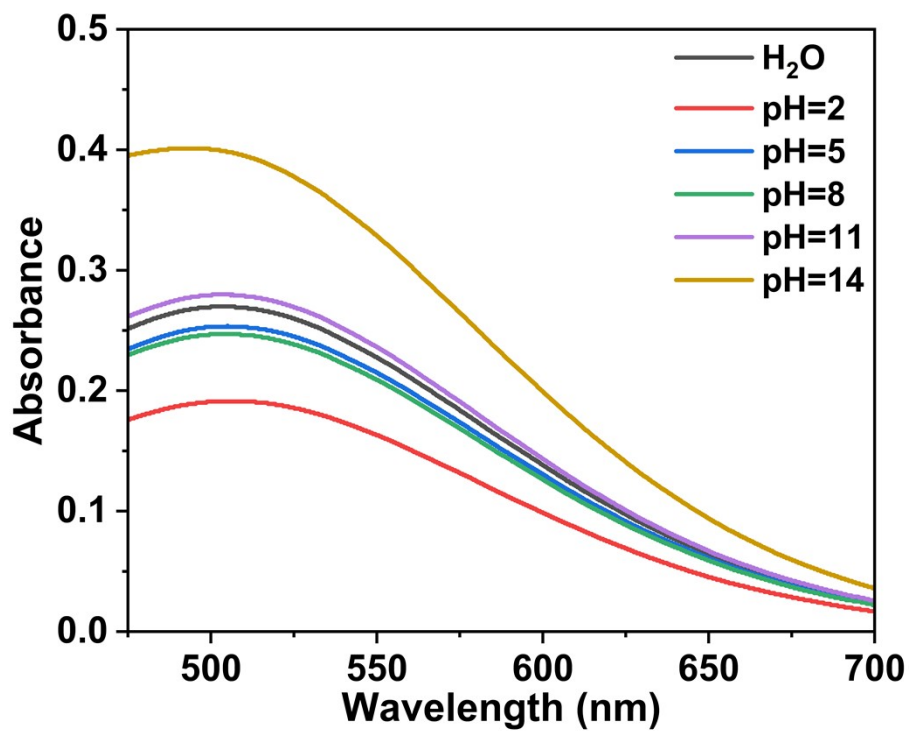


Fig. S4 UV-Vis spectra of DCU solution.



**Fig. S5** UV-Vis spectra of acetate derivative solution with varying ethanol concentration.



**Fig. S6** UV-Vis spectra of acetate derivative solution with varying pH.

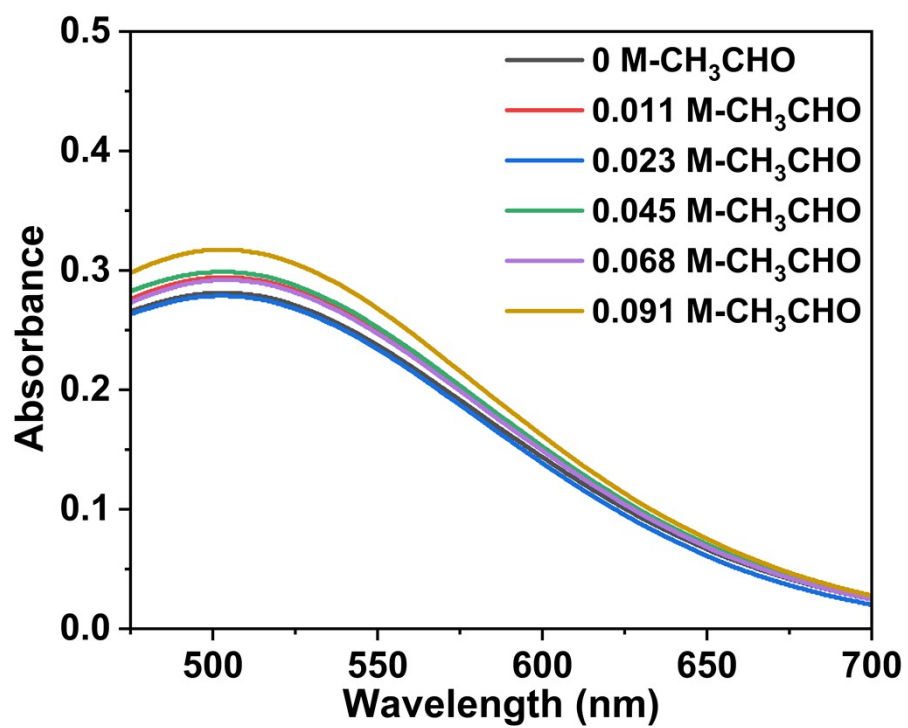


**Fig. S7** UV-Vis spectra of acetate derivative solution with varying acetaldehyde concentrations.

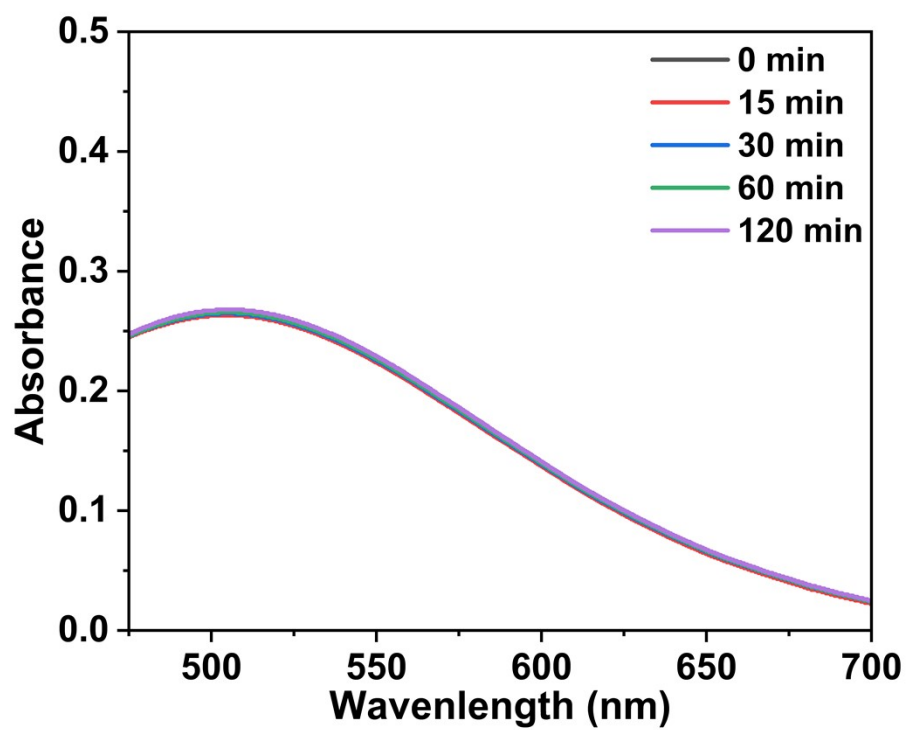


**Fig. S8** UV-Vis spectra of acetate derivative solution with varying time.

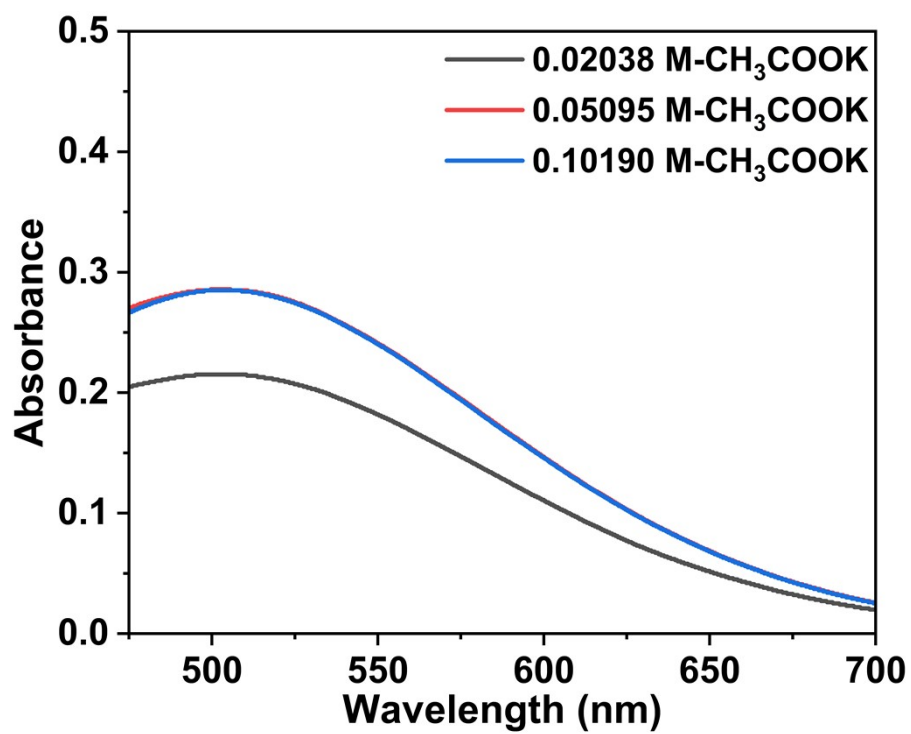


**Fig. S9** UV-Vis spectra of acetate derivative solution with different acetate concentrations in a mixed solution of  $1 \text{ mol}\cdot\text{L}^{-1}$  KOH +  $1 \text{ mol}\cdot\text{L}^{-1}$  ethanol.

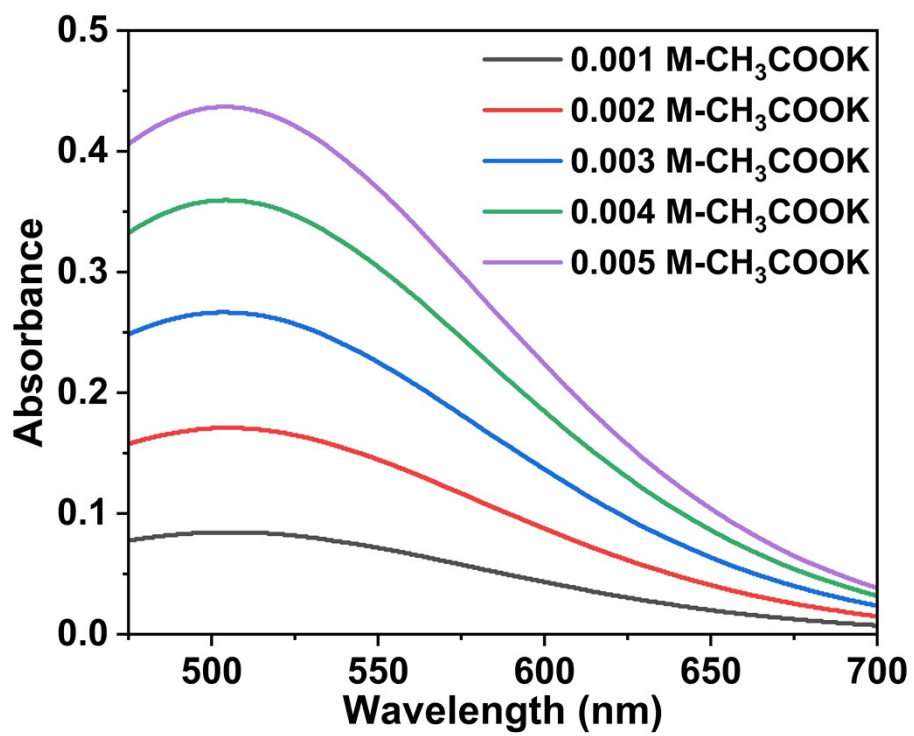


**Fig. S10** UV-Vis spectra of acetate derivative solution with varying acetate concentrations.

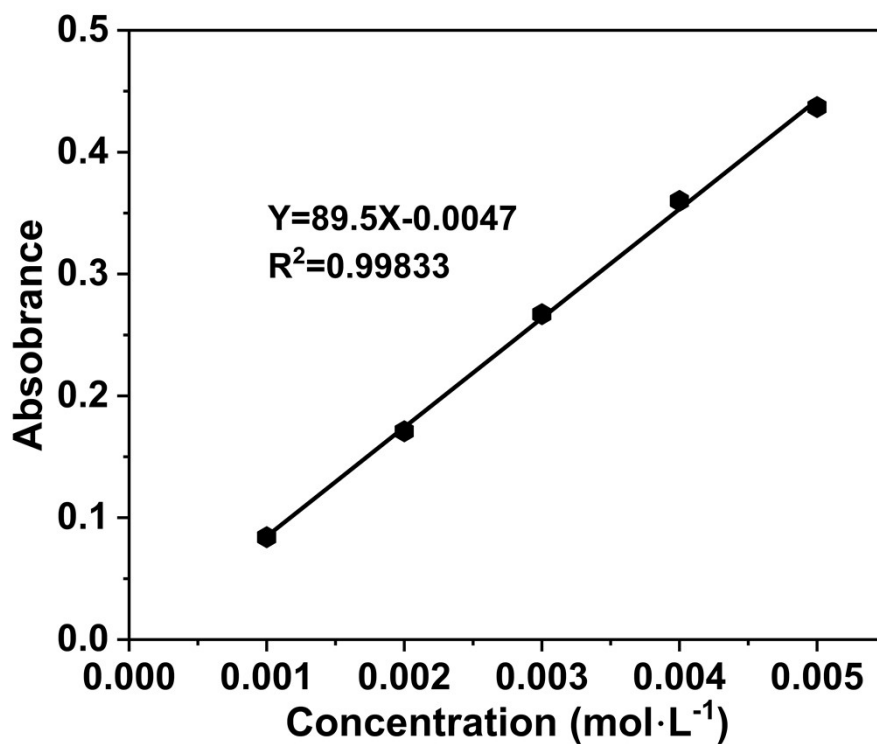


**Fig. S11** Linear relationship between absorbance at 505 nm and acetate concentrations (0.001–0.005 mol·L<sup>-1</sup>). The calibration curve was established by fitting the processed datasets shown in **Fig. S10**. This curve was subsequently applied to quantify acetate in real samples obtained at applied potentials of 1.47 and 1.52 V vs. RHE.

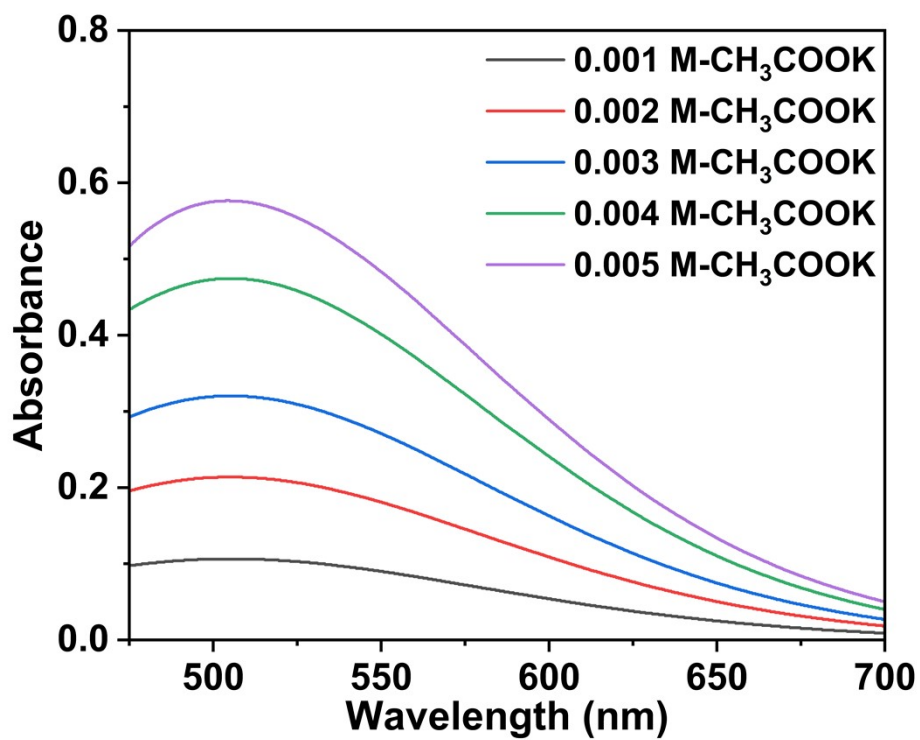


**Fig. S12** UV-Vis spectra of acetate derivative solution with varying acetate concentrations.

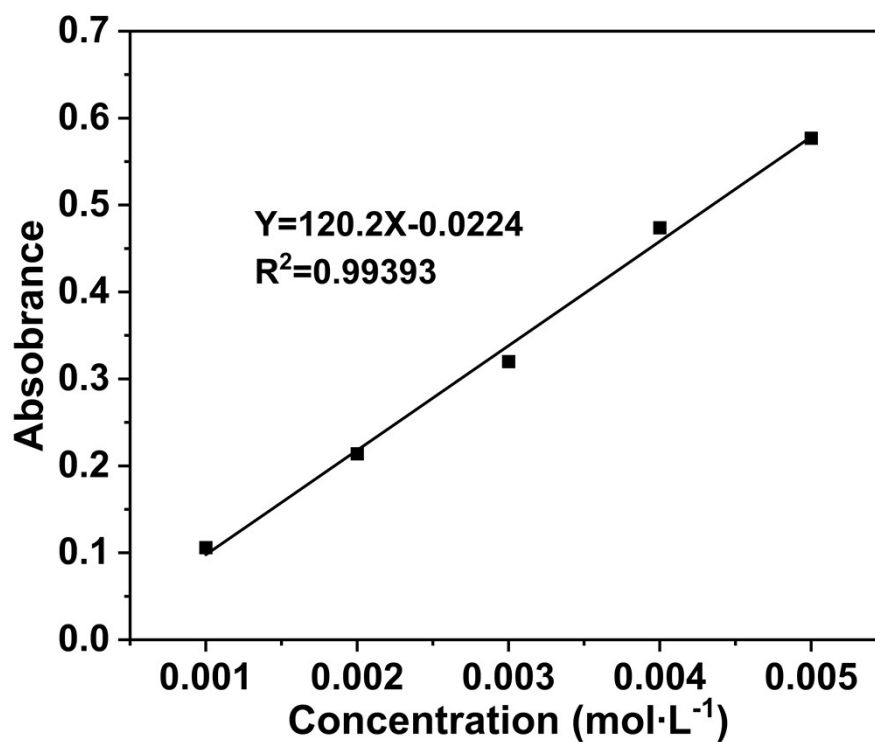


**Fig. S13** Linear relationship between absorbance at 505 nm and acetate concentrations (0.001–0.005 mol·L<sup>-1</sup>). The calibration curve was established by fitting the processed datasets shown in **Fig. S12**. This curve was subsequently applied to quantify acetate in real samples obtained at applied potentials of 1.42 and 1.57 V vs. RHE.

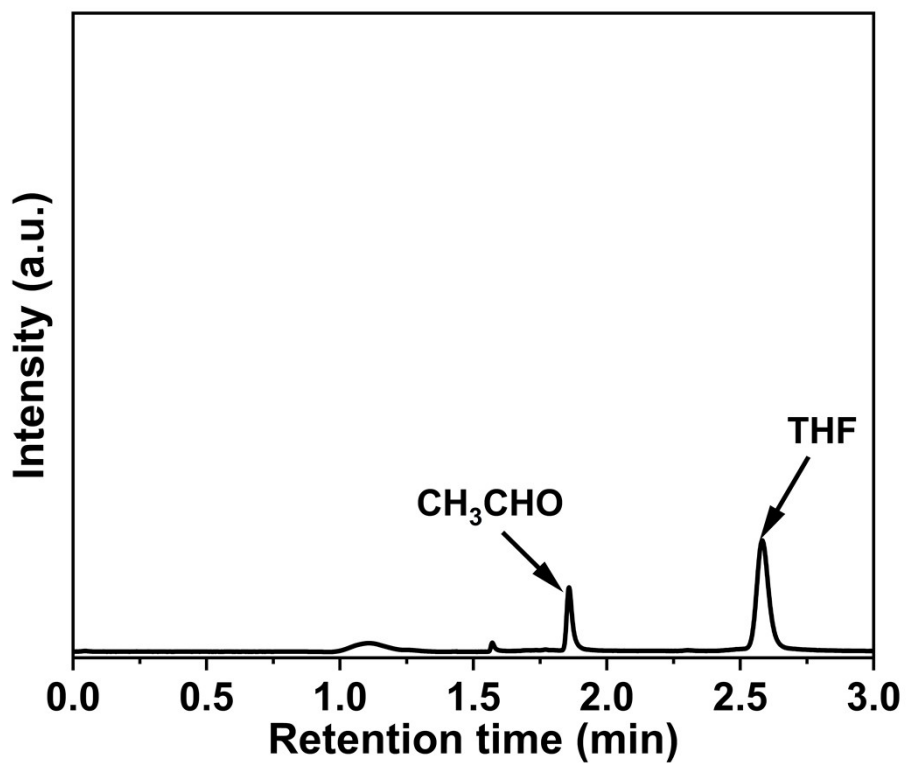


**Fig. S14** Gas chromatogram of  $0.1 \text{ mg}\cdot\text{g}^{-1}$  acetaldehyde using THF as an internal standard.

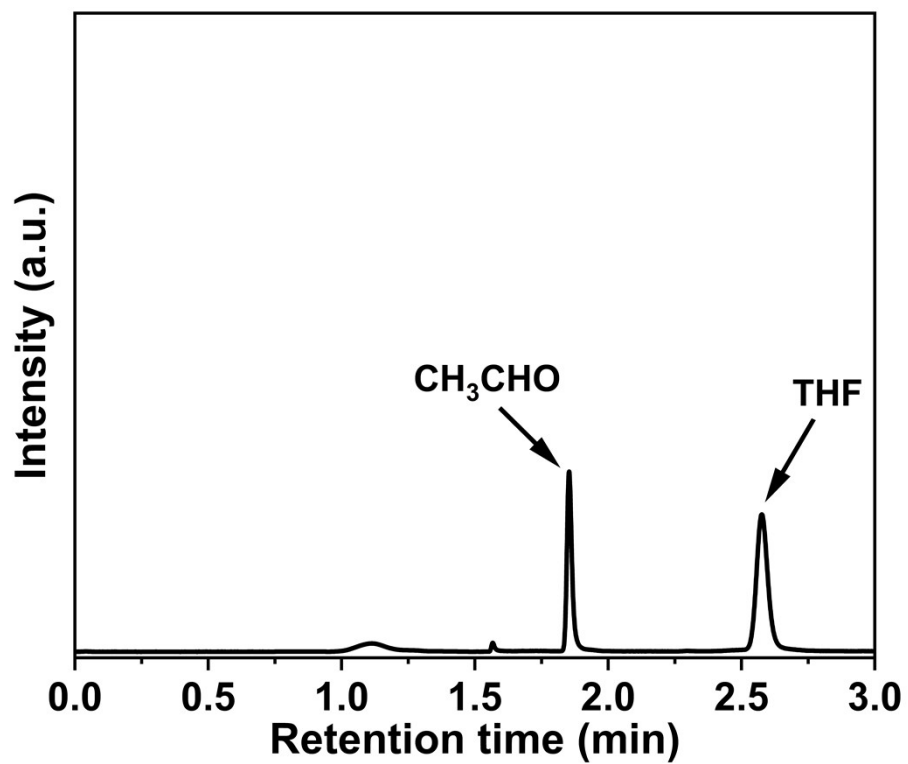


**Fig. S15** Gas chromatogram of  $0.2 \text{ mg}\cdot\text{g}^{-1}$  acetaldehyde using THF as an internal standard.

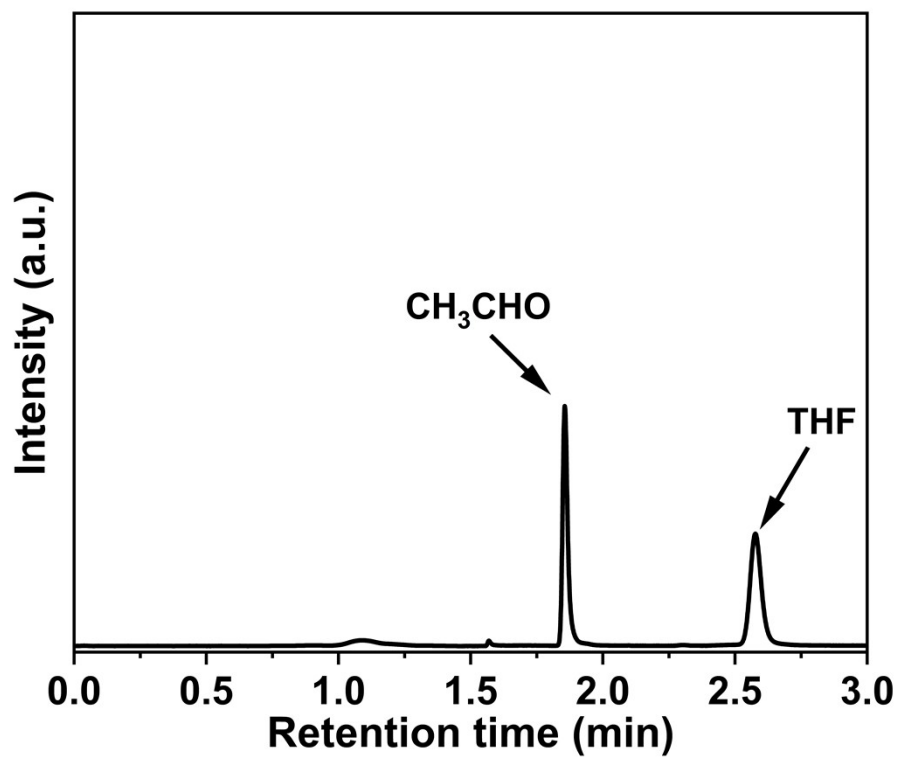


**Fig. S16** Gas chromatogram of  $0.3 \text{ mg}\cdot\text{g}^{-1}$  acetaldehyde using THF as an internal standard.

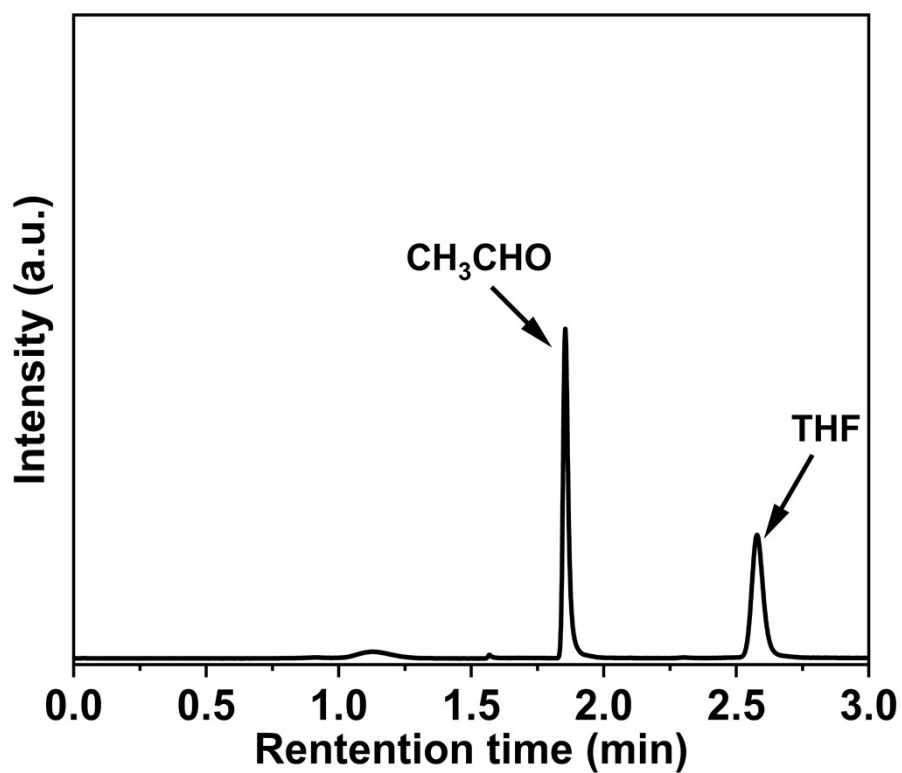


**Fig. S17** Gas chromatogram of  $0.4 \text{ mg}\cdot\text{g}^{-1}$  acetaldehyde using THF as an internal standard.

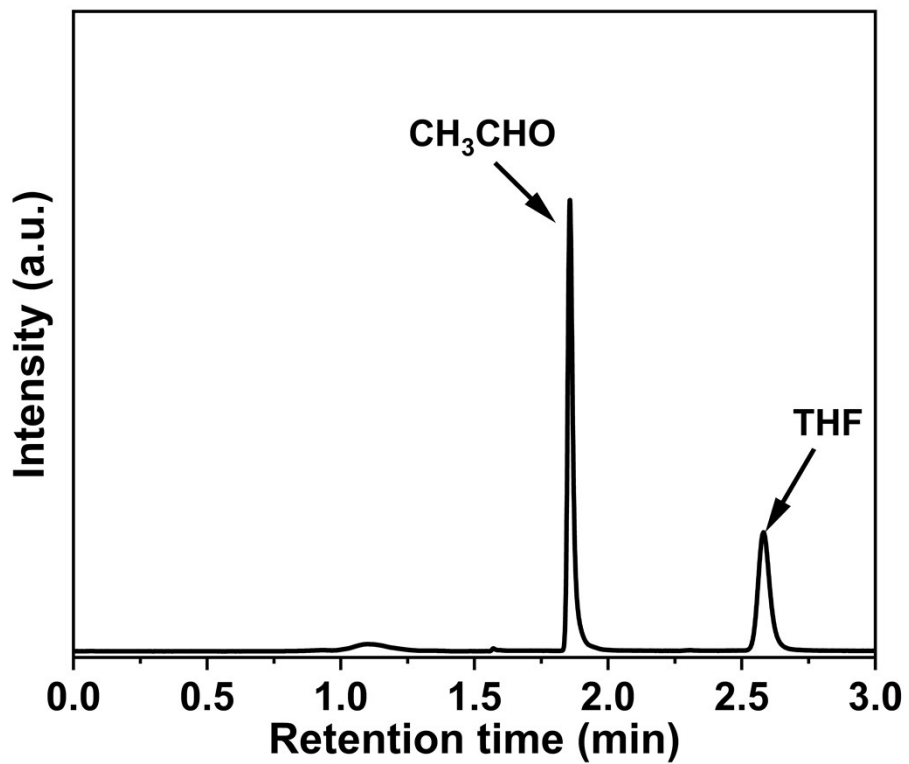


**Fig. S18** Gas chromatogram of  $0.5 \text{ mg}\cdot\text{g}^{-1}$  acetaldehyde using THF as an internal standard.

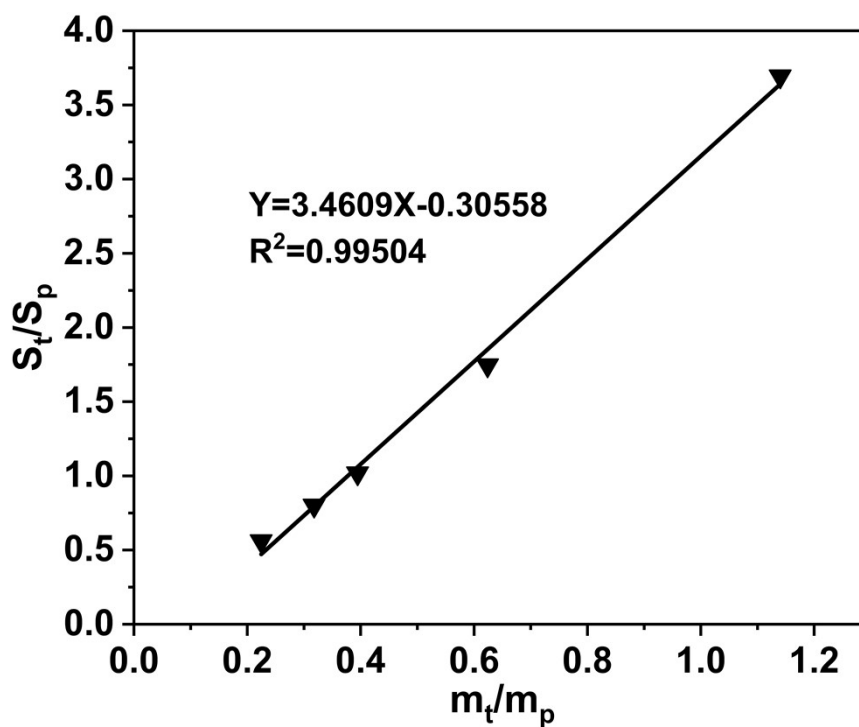


**Fig. S19** Linear relationship between  $m_t$  (internal standard mass)/ $m_p$  (product mass) and  $S_t$  (internal standard peak area)/ $S_p$  (product peak area). The calibration curve was established by fitting the processed datasets shown in **Fig. S14–S18**. This curve was subsequently applied to quantify acetaldehyde in real samples obtained at applied potentials of 1.47 and 1.52 V vs. RHE.

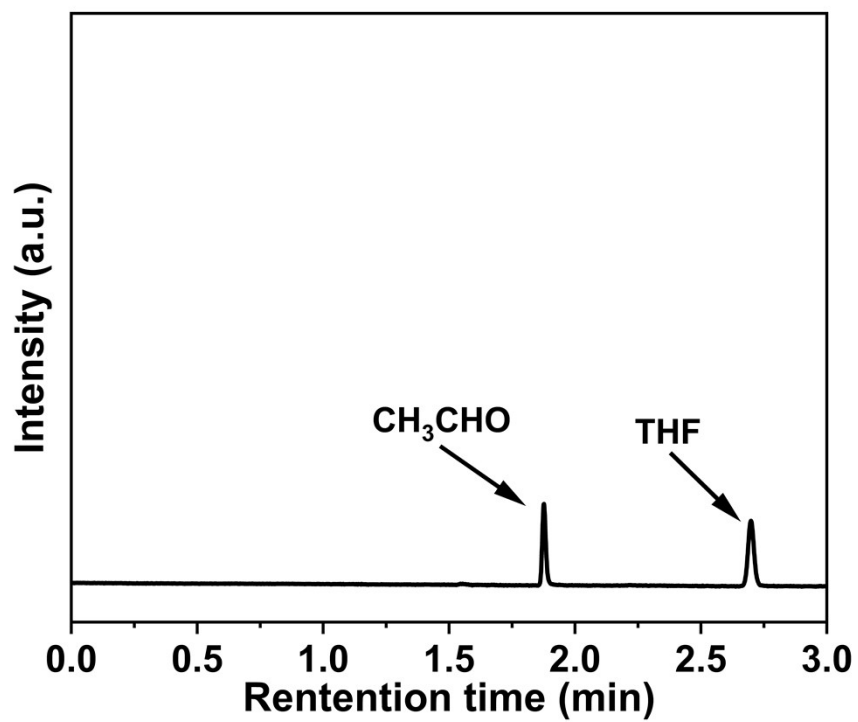


**Fig. S20** Gas chromatogram of 0.1 mg·g<sup>-1</sup> acetaldehyde using THF as an internal standard.

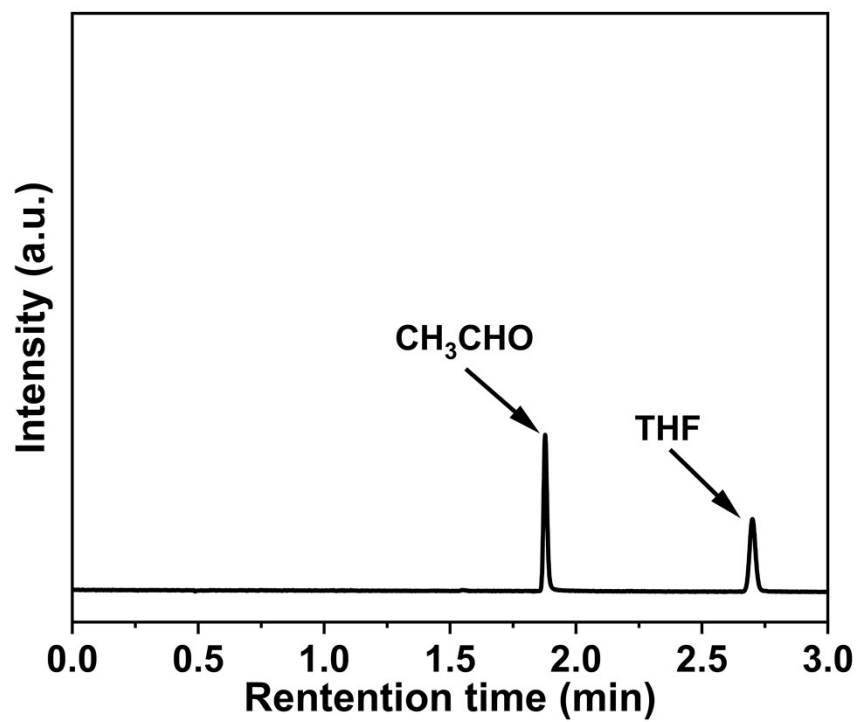


**Fig. S21** Gas chromatogram of  $0.2 \text{ mg}\cdot\text{g}^{-1}$  acetaldehyde using THF as an internal standard.

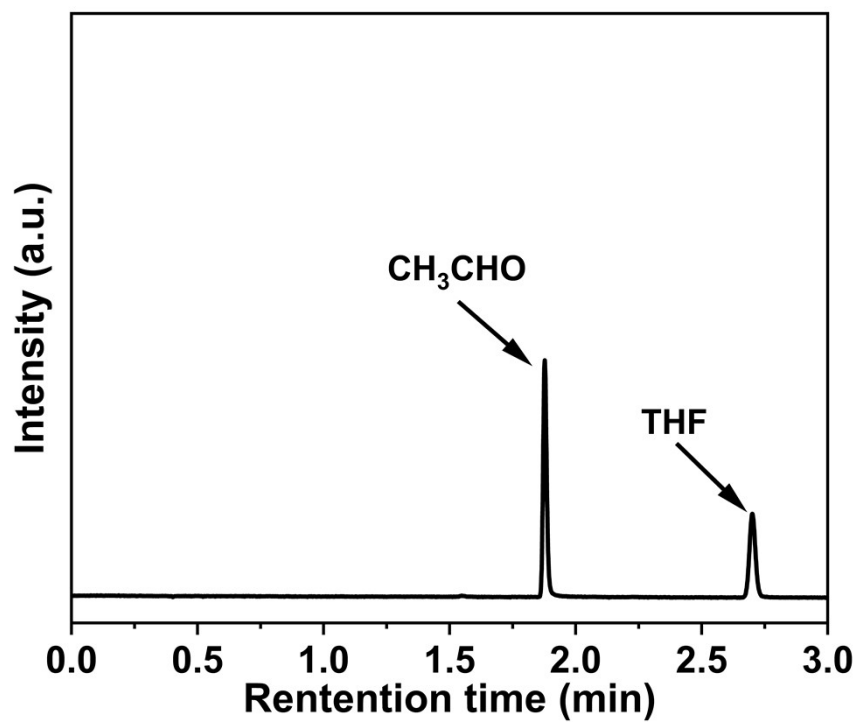


**Fig. S22** Gas chromatogram of  $0.3 \text{ mg}\cdot\text{g}^{-1}$  acetaldehyde using THF as an internal standard.

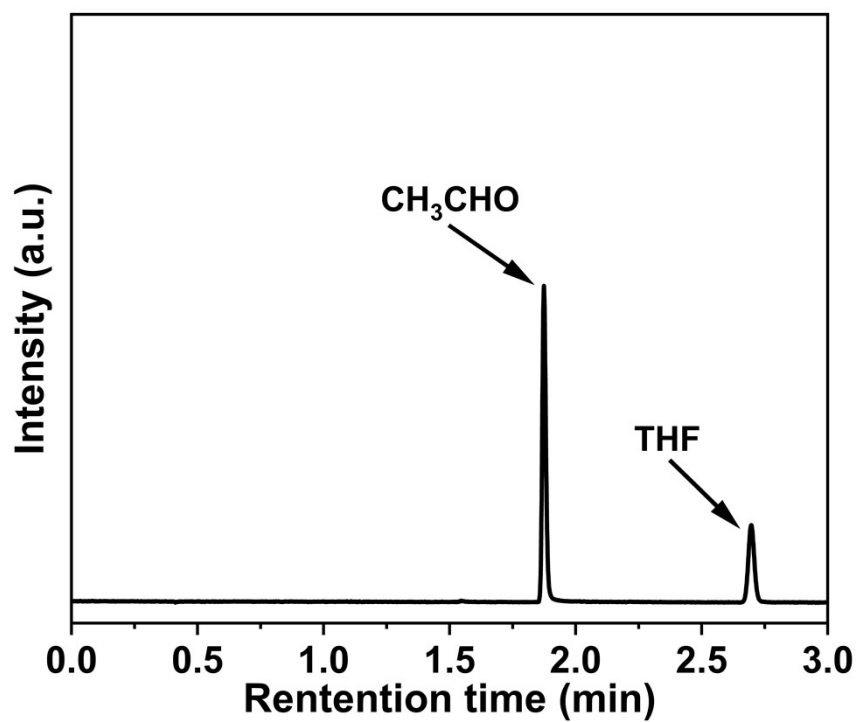


**Fig. S23** Gas chromatogram of 0.4 mg·g<sup>-1</sup> acetaldehyde using THF as an internal standard.

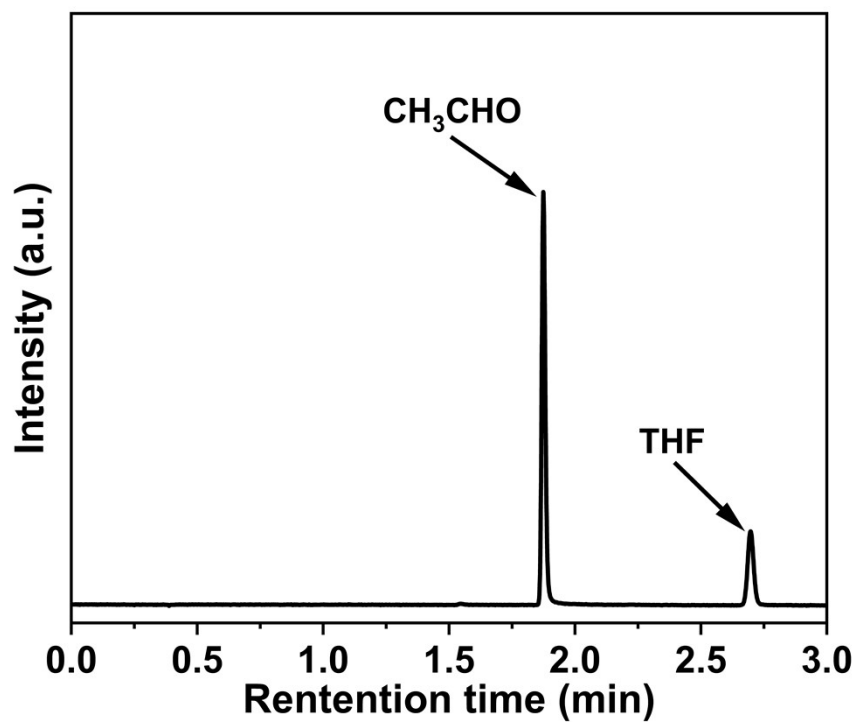


**Fig. S24** Gas chromatogram of  $0.5 \text{ mg}\cdot\text{g}^{-1}$  acetaldehyde using THF as an internal standard.

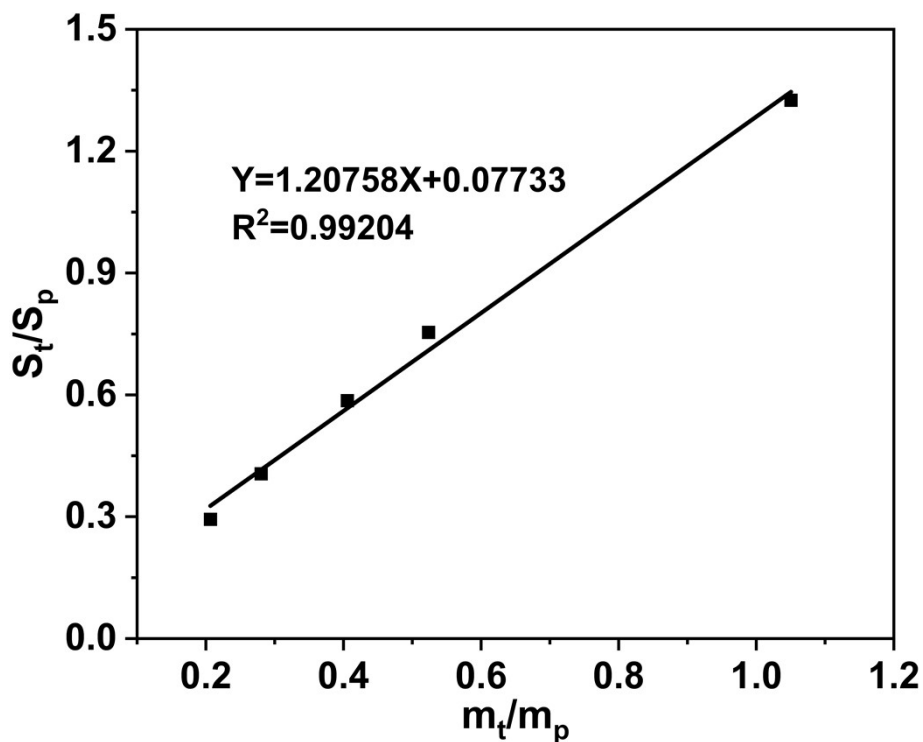


**Fig. S25** Linear relationship between  $m_t$  (internal standard mass)/ $m_p$  (product mass) and  $S_t$  (internal standard peak area)/ $S_p$  (product peak area). The calibration curve was established by fitting the processed datasets shown in **Fig. S20–S24**. This curve was subsequently applied to quantify acetaldehyde in real samples obtained at applied potentials of 1.42 and 1.57 V vs. RHE.

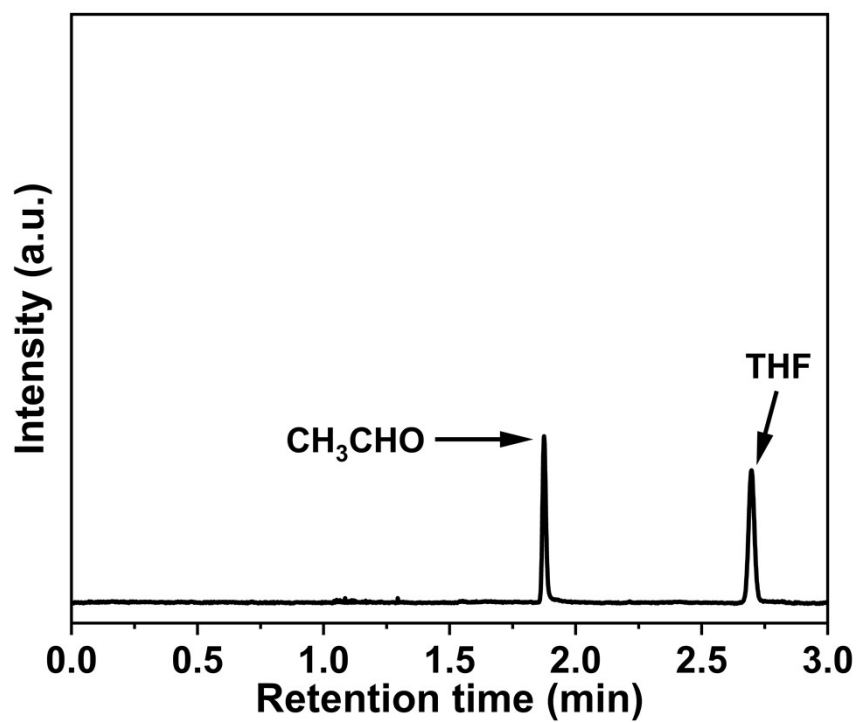


**Fig. S26** Gas chromatogram of acetaldehyde in the products generated at a potential of 1.42 vs. RHE using THF as an internal standard.

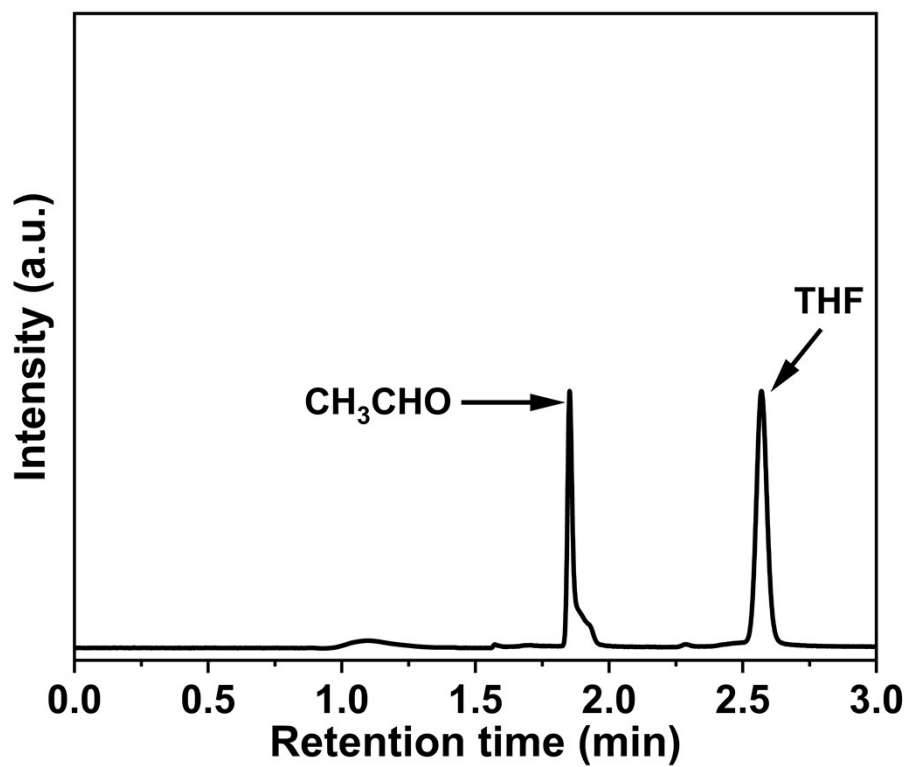


**Fig. S27** Gas chromatogram of acetaldehyde in the products generated at a potential of 1.47 vs. RHE using THF as an internal standard.

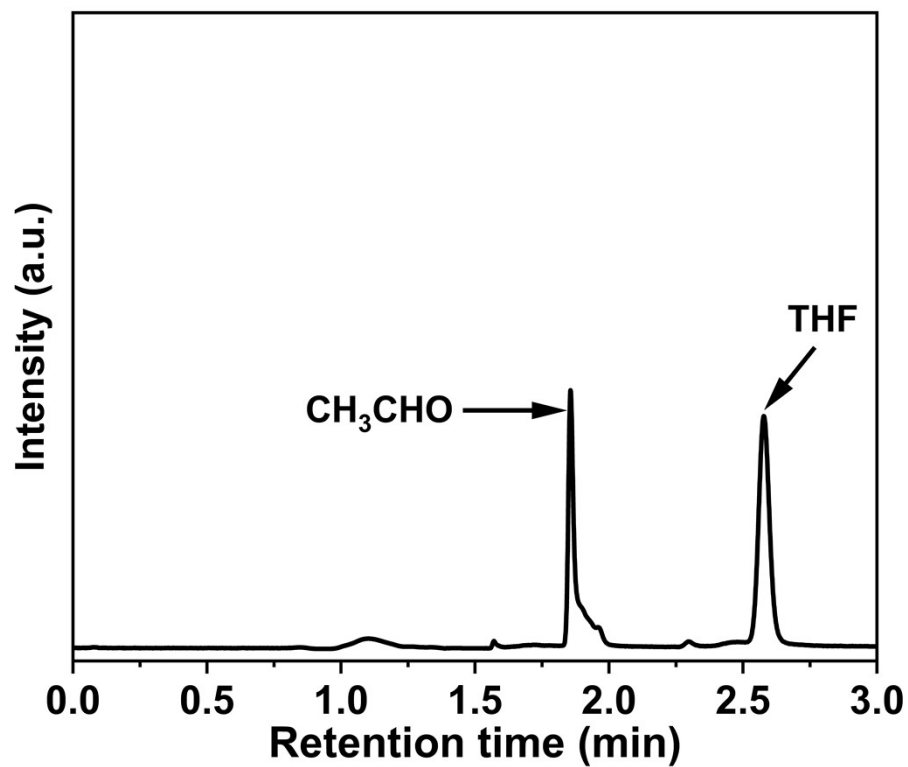


**Fig. S28** Gas chromatogram of acetaldehyde in the products generated at a potential of 1.52 vs. RHE using THF as an internal standard.

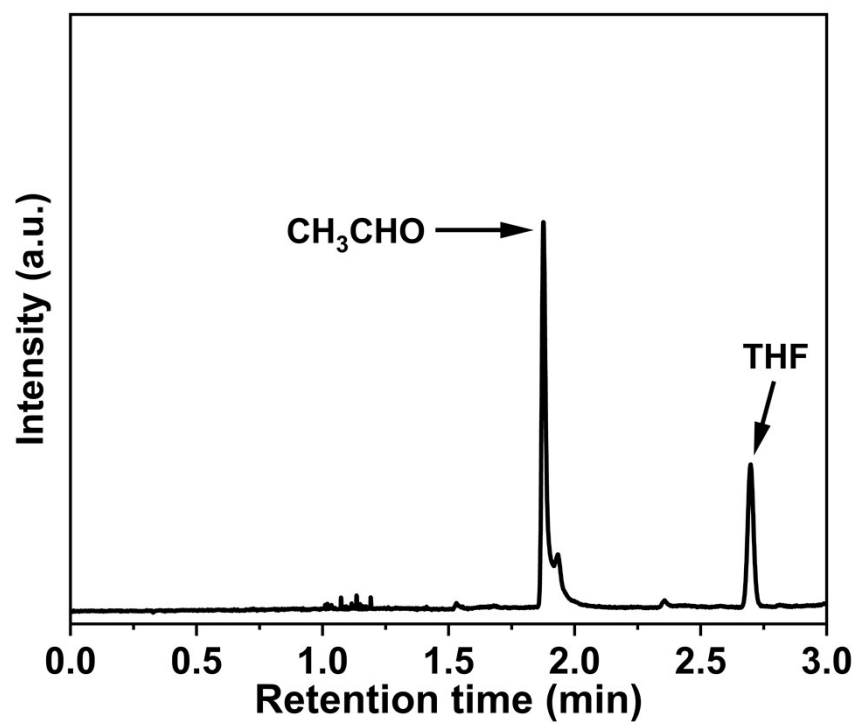


**Fig. S29** Gas chromatogram of acetaldehyde in the products generated at a potential of 1.57 vs. RHE using THF as an internal standard.

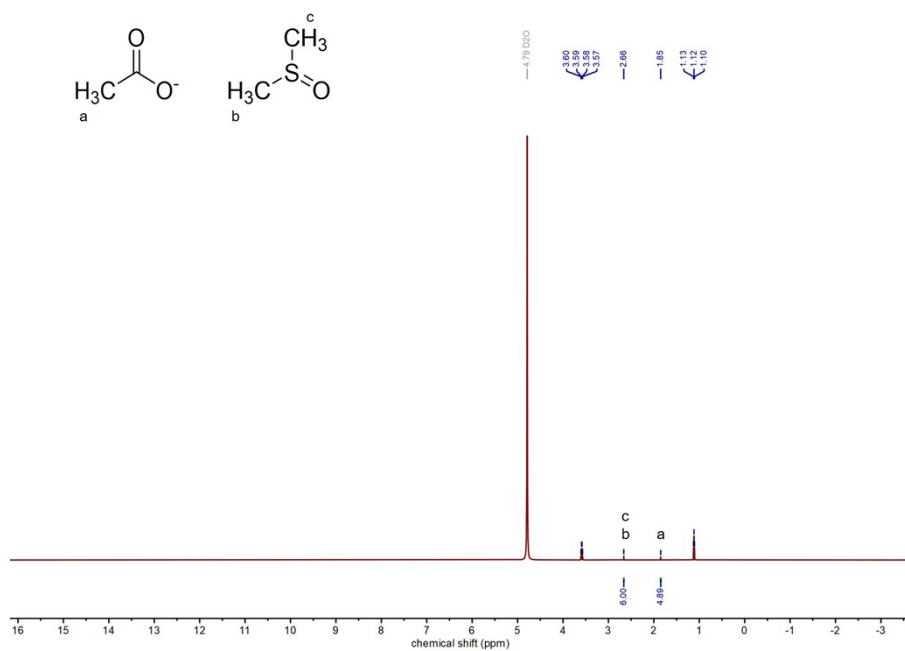


**Fig. S30**  $^1\text{H}$  NMR (600 MHz, 298 K) spectrum of the sample generated at 1.57 V vs. RHE, diluted fivefold with  $\text{D}_2\text{O}$ , using DMSO as an internal standard.

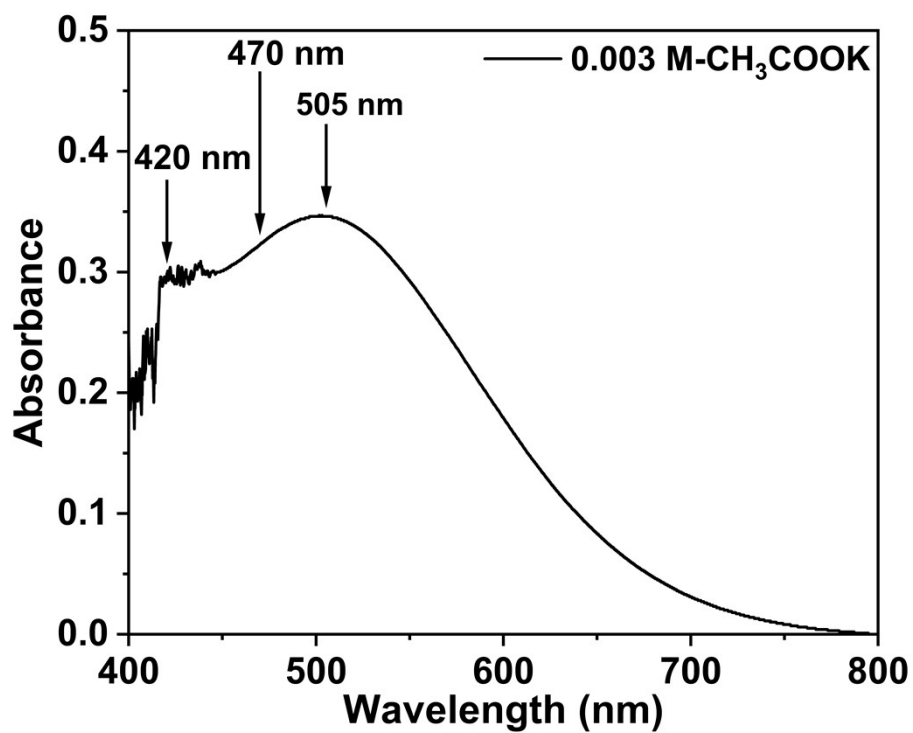


**Fig. S31** UV-Vis absorption spectra of a sample containing 0.003 mol·L<sup>-1</sup> acetate, 0.1 mol·L<sup>-1</sup> NH<sub>2</sub>OH·HCl, 0.4 mol·L<sup>-1</sup> DCC, and 0.3 mol·L<sup>-1</sup> FeCl<sub>3</sub>, reacted at 60 °C in a reaction.